

Transient pulsed radio emission from a magnetar

Fernando Camilo¹, Scott M. Ransom², Jules P. Halpern¹, John Reynolds³, David J. Helfand¹, Neil Zimmerman¹ & John Sarkissian³

¹ Columbia Astrophysics Laboratory, Columbia University, 550 West 120th Street, New York, New York 10027, USA.

² National Radio Astronomy Observatory, 520 Edgemont Road, Charlottesville, Virginia 22903, USA.

³ Australia Telescope National Facility, CSIRO, Parkes Observatory, PO Box 276, Parkes, New South Wales 2870, Australia.

Anomalous X-ray pulsars (AXPs) are slowly rotating neutron stars with very bright and highly variable X-ray emission that are believed to be powered by ultra-strong magnetic fields of $> 10^{14}$ G, according to the ‘magnetar’ model.¹ The radio pulsations that have been observed from more than 1,700 neutron stars with weaker magnetic fields have never been detected from any of the dozen known magnetars. The X-ray pulsar XTE J1810–197 was revealed (in 2003) as the first AXP with transient emission when its luminosity increased 100-fold from the quiescent level²; a coincident radio source of unknown origin was detected one year later.³ Here we show that XTE J1810–197 emits bright, narrow, highly linearly polarized radio pulses, observed at every rotation, thereby establishing that magnetars can be radio pulsars. There is no evidence of radio emission before the 2003 X-ray outburst (unlike ordinary pulsars, which emit radio pulses all the time), and the flux varies from day to day. The flux at all radio frequencies is approximately equal — and at > 20 GHz XTE J1810–197 is currently the brightest neutron star known. These observations link magnetars to ordinary radio pulsars, rule out alternative accretion models for AXPs, and provide a new window into the coronae of magnetars.

We observed the position of XTE J1810–197 (ref. 4) on 17 March 2006 for 4.2 hours with the Parkes telescope at a central frequency $\nu = 1.4$ GHz, using parameters identical to those used in the Parkes multibeam pulsar survey.⁵ Pulsations with period $P = 5.54$ s were easily detected, with period-averaged flux density $S_{1.4} = 6$ mJy and a narrow average profile with full-width at half-maximum of 0.15 s (Fig. 1). We detected individual pulses from virtually every rotation of the neutron star (see Fig. 2). These are composed of $\lesssim 10$ -ms-wide sub-pulses with peak flux densities up to $\gtrsim 10$ Jy and follow a differential flux distribution approximated by $d \log N = -d \log S$, with no giant pulses like those observed from the Crab pulsar.⁶

A timing model accounting for every turn of the neutron star during the period 17 March–7 May yields barycentric $P = 5.54024870$ s ± 20 ns on MJD 53855.0 and $\dot{P} = (1.016 \pm 0.001) \times 10^{-11}$, with root-mean-square residual $\sigma = 5$ ms. We use this to set constraints on any putative companion to the AXP by requiring the light-travel-time across the projected orbital semi-major axis to be less than σ . From Kepler’s third law, with assumed neutron star mass $1.4 M_{\odot}$, the upper limits on the minimum companion mass lie in the range ~ 0.003 – $0.03 M_{\odot}$ for orbital periods in the range 2 h–5 min, effectively ruling out the existence of any Roche lobe-filling star orbiting this AXP. The delay in pulse arrival times measured between 2.9 and 0.7 GHz implies an integrated column density of free electrons between the Earth and XTE J1810–197 of

$178 \pm 5 \text{ cm}^{-3} \text{ pc}$. Together with a model for the Galactic distribution of free electrons,⁷ the distance to XTE J1810–197 is $D \approx 3.3$ kpc (here we use \approx to indicate a quantity known to within about a factor of two or better), consistent with X-ray- and optically-derived estimates of 2.5–5 kpc (refs 8–10).

In the original detection of radio emission from XTE J1810–197 with the Very Large Array (VLA) in January 2004, $S_{1.4} = 4.5$ mJy (ref. 3). In February 2006 at the VLA we measured $S_{1.4} = 12.9$ mJy, a considerable increase in flux over a period of two years. However, further observations (see Table 1) reveal large fluctuations: at Parkes, $S_{1.4}$ can vary by factors of about two from one day to the next, although no significant variations are detected within observing sessions lasting up to four hours. These flux variations are completely inconsistent with expectations from interstellar scintillation^{11,12} and are thus, remarkably for a pulsar, intrinsic to XTE J1810–197. At the VLA, $S_{8.4}$ shows variations by similar factors within 20 min. This more rapid variation at high frequencies is confirmed in pulsed observations with the Green Bank Telescope (GBT). However, at $\nu \gtrsim 9$ GHz diffractive interstellar scintillation^{11,12} plays a significant role.⁷ At present we cannot rule out a non-pulsed component. The maximum size of any extended emission is $5 \times 10^{15} (D/3 \text{ kpc}) \text{ cm}$, based on the 0.25-arcsec resolution of our VLA image at 8.4 GHz, from which we measure a position for XTE J1810–197 of right

ascension = 18 h 09 min 51.087 s \pm 0.001 s and declination = $-19^{\circ} 43' 51.93'' \pm 0.02''$, in the J2000.0 equinox.

The radio spectrum of XTE J1810–197 is quite flat over a factor of 60 in frequency. We have made independent simultaneous measurements of flux at multiple frequencies (see Table 1), all of which are consistent with spectral index $\alpha \gtrsim -0.5$, where $S_{\nu} \propto \nu^{\alpha}$. Ordinary pulsars have mean $\alpha = -1.6$, and fewer than 10% have $\alpha > -0.5$ (ref. 13). With an unremarkable average flux at $\nu \sim 1$ GHz (here we use \sim to indicate a quantity known to within about an order of magnitude), by $\nu \gtrsim 20$ GHz, XTE J1810–197 is brighter than every other known neutron star. Its assumed isotropic radio luminosity up to 42 GHz is about 2×10^{30} erg s $^{-1}$, compared to the spin-down luminosity of about 2.4×10^{33} erg s $^{-1}$.

Radiation from XTE J1810–197 is highly polarized: $89 \pm 5\%$ of the total-intensity 8.4-GHz flux measured at the VLA is linearly polarized. Also, a 1.4-GHz Parkes observation shows linear polarization that tracks the total-intensity pulse profile at a level of 65%.

XTE J1810–197 is located within the boundaries of the Parkes multibeam pulsar survey area.⁵ We have analysed archival raw survey data from the two telescope pointings nearest to the pulsar position. No pulsar signal was detected in average-pulse analyses, corresponding to $S_{1.4} \lesssim 0.2$ mJy from these observations made in 1997 and 1998 (see Table 1). This limit is $< 10\%$ of the flux from the pulsar since 2004, suggesting that the extraordinary radio emission from XTE J1810–197 turned on as a result of the events accompanying the X-ray outburst observed in early 2003 (ref. 2).

However, about 10% of ordinary pulsars have specific radio luminosity $L_{1.4} \equiv S_{1.4} D^2 \lesssim 2$ mJy kpc 2 , the approximate limit for XTE J1810–197 before the outburst. For example, the pulsar PSR J1718–3718, with $L_{1.4} \approx 4$ mJy kpc 2 and $P = 3.3$ s, has inferred surface dipole magnetic field strength $B = 7 \times 10^{13}$ G, higher than that of one magnetar (for XTE J1810–197, $B \approx 2.4 \times 10^{14}$ G). This source has X-ray properties apparently similar to those of XTE J1810–197 in quiescence.¹⁴ This raises the prospect that XTE J1810–197 could have generated familiar radio pulsar emission before 2003, marking a plausible direct link between ordinary pulsars and magnetars. In addition, a recently discovered class of radio-bursting neutron stars¹⁵ includes at least one object whose field strength is comparable to that of some magnetars; it too has X-ray properties resembling those of XTE J1810–197 in quiescence.¹⁶ We therefore also searched the archival radio data for bright individual pulses, but found none.

Observable magnetospheric radio emission requires a coherent mechanism, inferred to be curvature radiation whose characteristic frequency $3\gamma^3 c/4\pi r$ falls in the gigahertz range for secondary particle Lorentz factors $\gamma \sim 10^3$ and radii of curvature r of the order of the light-cylinder radius $r_{lc} = cP/2\pi$ or smaller. In ordinary pulsars, the required electron–positron pairs can be produced only on

the open field-line bundle at high altitude above the surface where electric potentials of $\sim 10^{12}$ V accelerate particles that emit gamma-rays with energies exceeding the pair-creation threshold. We cannot exclude that the handful of known magnetars employ this mechanism, because their long periods imply small active polar caps and narrow beams that may miss the observer for random orientations. Additionally, magnetars have mechanisms and locations for pair creation that are not available to ordinary pulsars.^{17–19} Magnetar activity is generated by the sudden or continual twisting of the external field lines into a non-potential configuration that maintains, by induction, strong long-lived currents flowing along them.²⁰ With required charge densities greatly exceeding the corotation value²¹ for a dipole field, an electric potential of $\sim 10^9$ V is established and self-regulated by pair creation. In these conditions, electrons and positrons are accelerated to $\gamma \sim 10^3$, and pairs can be created either via resonant cyclotron scattering of thermal X-rays in the strong magnetic field or thermally in the heated atmosphere at the footpoints of the twisted field lines. This affords the possibility that magnetar radio emission is generated on closed field lines and beamed into a wide range of angles. Because most of the energy of the twisted field is contained within a few stellar radii, the frequencies of coherent emission from magnetars could be greater than those of ordinary pulsars, possibly accounting for the flat radio spectrum of XTE J1810–197. Also, it has been proposed that the observed optical and infrared emission from magnetars is coherent emission from plasma instabilities above the plasma frequency,^{22,23} and even that radio or submillimetre emission could be so generated.²⁴ The extrapolated radio spectrum of XTE J1810–197 exceeds its observed infrared fluxes,²⁵ so that the radio and infrared emission may or may not have the same origin.

Radio emission as currently observed from XTE J1810–197 was evidently not present during the historical quiescent X-ray state that persisted for at least 24 years before the outburst.²⁶ Following this, the onset of radio emission could have been delayed until the plasma density declined to a value much less than is generally found in persistent magnetars. The hard and soft X-ray fluxes are now decaying exponentially with timescales of ≈ 300 and ≈ 900 days, respectively,⁸ while strong radio emission is still observed more than three years after the X-ray turn-on. We infer that radio emission will cease after the transient X-ray components (and implied magnetospheric currents) have subsided, but it is difficult to know whether this transition is imminent, or will take many years.

Received 12 May; accepted 14 June 2006.

1. Duncan, R. C. & Thompson, C. Formation of very strongly magnetized neutron stars: implications for gamma-ray bursts. *Astrophys. J.* **392**, L9–L13 (1992).
2. Ibrahim, A. I. *et al.* Discovery of a transient magnetar: XTE J1810–197. *Astrophys. J.* **609**, L21–L24 (2004).

3. Halpern, J. P., Gotthelf, E. V., Becker, R. H., Helfand, D. J. & White, R. L. Discovery of radio emission from the transient anomalous X-ray pulsar XTE J1810–197. *Astrophys. J.* **632**, L29–L32 (2005).
4. Israel, G. L. *et al.* Accurate X-ray position of the anomalous X-ray pulsar XTE J1810–197 and identification of its likely infrared counterpart. *Astrophys. J.* **603**, L97–L100 (2004).
5. Manchester, R. N. *et al.* The Parkes multi-beam pulsar survey — I. Observing and data analysis systems, discovery and timing of 100 pulsars. *Mon. Not. R. Astron. Soc.* **328**, 17–35 (2001).
6. Cordes, J. M., Bhat, N. D. R., Hankins, T. H., McLaughlin, M. A. & Kern, J. The brightest pulses in the Universe: multifrequency observations of the Crab pulsar’s giant pulses. *Astrophys. J.* **612**, 375–388 (2004).
7. Cordes, J. M. & Lazio, T. J. W. NE2001. I. A new model for the Galactic distribution of free electrons and its fluctuations. Preprint at <http://arxiv.org/astro-ph/0207156> (2002).
8. Gotthelf, E. V. & Halpern, J. P. The spectral evolution of transient anomalous X-ray pulsar XTE J1810–197. *Astrophys. J.* **632**, 1075–1085 (2005).
9. Gotthelf, E. V., Halpern, J. P., Buxton, M. & Bailyn, C. Imaging X-ray, optical, and infrared observations of the transient anomalous X-ray pulsar XTE J1810–197. *Astrophys. J.* **605**, 368–377 (2004).
10. Durant, M. & van Kerkwijk, M. H. Distances to anomalous X-ray pulsars using red clump stars. *Astrophys. J.* (in the press); preprint at <http://arxiv.org/astro-ph/0606027> (2006).
11. Rickett, B. J. Radio propagation through the turbulent interstellar plasma. *Annu. Rev. Astron. Astrophys.* **28**, 561–605 (1990).
12. Narayan, R. The physics of pulsar scintillation. *Phil. Trans. R. Soc. A* **341**, 151–165 (1992).
13. Lorimer, D. R., Yates, J. A., Lyne, A. G. & Gould, D. M. Multifrequency flux density measurements of 280 pulsars. *Mon. Not. R. Astron. Soc.* **273**, 411–421 (1995).
14. Kaspi, V. M. & McLaughlin, M. A. Chandra X-ray detection of the high-magnetic-field radio pulsar PSR J1718–3718. *Astrophys. J.* **618**, L41–L44 (2005).
15. McLaughlin, M. A. *et al.* Transient radio bursts from rotating neutron stars. *Nature* **439**, 817–820 (2006).
16. Reynolds, S. P. *et al.* Discovery of the X-ray counterpart to the rotating radio transient J1819–1458. *Astrophys. J.* **639**, L71–L74 (2006).
17. Thompson, C. & Beloborodov, A. M. High-energy emission from magnetars. *Astrophys. J.* **634**, 565–569 (2005).
18. Beloborodov, A. M. & Thompson, C. Corona of magnetars. *Astrophys. J.* (submitted); preprint at <http://arxiv.org/astro-ph/0602417> (2006).
19. Zhang, B. On the radio quiescence of anomalous X-ray pulsars and soft gamma-ray repeaters. *Astrophys. J.* **562**, L59–L62 (2001).
20. Thompson, C., Lyutikov, M. & Kulkarni, S. R. Electrodynamics of magnetars: implications for the persistent X-ray emission and spin-down of the soft gamma repeaters and anomalous X-ray pulsars. *Astrophys. J.* **574**, 332–355 (2002).
21. Goldreich, P. & Julian, W. H. Pulsar electrodynamics. *Astrophys. J.* **157**, 869–880 (1969).
22. Eichler, D., Gedalin, M. & Lyubarsky, Y. Coherent emission from magnetars. *Astrophys. J.* **578**, L121–L124 (2002).
23. Eichler, D., Lyubarsky, Y., Thompson, C. & Woods, P. M. In *Pulsars, AXPs and SGRs Observed with BeppoSAX and Other Observatories* (eds Cusumano, G., Massaro, E. & Mineo, T.) 215–222 (Aracne Editrice, Rome, 2003).
24. Lyutikov, M. Radio emission from magnetars. *Astrophys. J.* **580**, L65–L68 (2002).
25. Rea, N. *et al.* Correlated infrared and X-ray variability of the transient anomalous X-ray pulsar XTE J1810–197. *Astron. Astrophys.* **425**, L5–L8 (2004).
26. Halpern, J. P. & Gotthelf, E. V. The fading of transient anomalous X-ray pulsar XTE J1810–197. *Astrophys. J.* **618**, 874–882 (2005).
27. Backer, D. C. Peculiar pulse burst in PSR 1237+25. *Nature* **228**, 1297–1298 (1970).
28. Backer, D. C. *et al.* A digital signal processor for pulsar research. *Publ. Astron. Soc. Pacif.* **109**, 61–68 (1997).
29. Kaplan, D. L. *et al.* The Green Bank Telescope pulsar Spigot. *Publ. Astron. Soc. Pacif.* **117**, 643–653 (2005).
30. Drake, F. D. & Craft, H. D. Second periodic pulsations in pulsars. *Nature* **220**, 231–235 (1968).

Acknowledgements We thank J. Cohen and B. Mason for giving us some of their observing time, M. Kramer and M. McLaughlin for providing us with Parkes multibeam survey archival data, and D. Backer, D. Kaplan, and B. Jacoby for their contributions to developing pulsar observing equipment at GBT. The Parkes Observatory is part of the Australia Telescope, which is funded by the Commonwealth of Australia for operation as a National Facility managed by CSIRO. The National Radio Astronomy Observatory is a facility of the US National Science Foundation (NSF), operated under cooperative agreement by Associated Universities, Inc. F.C. acknowledges support from NSF and NASA.

Author Information Reprints and permissions information is available at npg.nature.com/reprintsandpermissions. The authors declare no competing financial interests. Correspondence and requests for materials should be addressed to F.C. (fernando@astro.columbia.edu).

Instrument	Frequency, ν (GHz)	Date (MJD)	Flux density, S_ν (mJy)
Parkes	1.4	50747	$\lesssim 0.25$
Parkes	1.4	51152	$\lesssim 0.15$
VLA	1.4	53019	4.5 ± 0.5
VLA	1.4	53794	12.9 ± 0.2
Parkes	1.4	53811	6.0
Parkes	1.4	53850.9 ^a	6.8
Parkes	1.4	53851.9	13.6
Parkes	1.4	53852.9	13.2
Parkes	1.4	53855.9 ^b	8.7
GBT (BCPM)	1.4	53862.4	5.1
Parkes	1.4	53862.9	7.8
VLA	1.4	53872	3.3 ± 0.2
VLA	1.4	53874	6.6 ± 0.5
VLA	1.4	53875	4.5 ± 0.5
VLA	1.4	53877	8.6 ± 0.7
VLA	1.4	53879	5.8 ± 0.6
GBT (BCPM)	1.9	53857.3 ^c	6.3
GBT (BCPM)	1.9	53865	6.0
Parkes	0.69	53850.9 ^a	7.4
GBT (BCPM)	0.82	53861.2	5.5
Parkes	2.9	53850.9 ^a	7.4
Parkes	6.4	53855.9 ^b	3.9
VLA	8.4	53828	9.0 ± 0.1
GBT (BCPM)	9.0	53857.4 ^c	3.0
GBT (BCPM)	14	53857.4 ^c	2.1
GBT (Spigot)	19	53857.5 ^c	1.9
GBT (Spigot)	42	53858.4	5.9

Table 1. Variable radio flux densities of XTE J1810–197. We list the flux densities from all observations of XTE J1810–197 with Parkes and GBT, as well as detections with the VLA (see also ref. 3). The X-ray outburst from XTE J1810–197 occurred between MJDs 52595 and 52662 (ref. 2). We searched for pulsations from the two pointings nearest to the neutron star in the Parkes multibeam pulsar survey⁵ (offset by 8 and 5 arcmin, respectively, where the telescope beam has full-width at half-maximum of 14.5 arcmin). A null result provides the given upper limits. Multiple observations at 1.4 and 1.9 GHz are listed by frequency chronologically in order to aid characterization of flux variations. Following this, we list observations in order of ascending frequency. VLA data are flux-calibrated with high precision using the flux density standard 3C286. Parkes and GBT fluxes are measured using the radiometer equation by comparing the area under each average pulse profile to the root-mean-square baseline and adopting known observing system characteristics. Absolute uncertainties for these fluxes are typically about 30% for $\nu \lesssim 9$ GHz, but increase for $\nu \geq 14$ GHz (we have applied corrections to account for the opacity of the atmosphere). Owing to poor atmospheric conditions, S_{42} is known to within a factor of only about 2. Relative changes in $S_{1.4}$ can be gauged with approximately 10% uncertainty, and clear variations (by factors of ≈ 2 on timescales of ~ 1 day) are observed at Parkes and also at VLA. On timescales typically up to one hour there is no evidence for intra-day variations in flux from any observation at $\nu \lesssim 9$ GHz. Conversely, all observations above this frequency show evidence for variability on timescales of several minutes. For example, on MJD 53828, $S_{8.4}$ was measured in successive 13-min scans across a 100-MHz band to be 7.4, 11.2, 9.6, 10.5, 5.1, and 8.3 mJy (all uncertainties ≤ 0.2 mJy). At these high frequencies, diffractive interstellar scintillation^{11,12} is at least partly responsible⁷ for the observed flux variations. We denote by superscripts a, b and c the three days on which we obtained multi-frequency data, from which the spectral index can be estimated with some accuracy: $\alpha \gtrsim -0.5$.

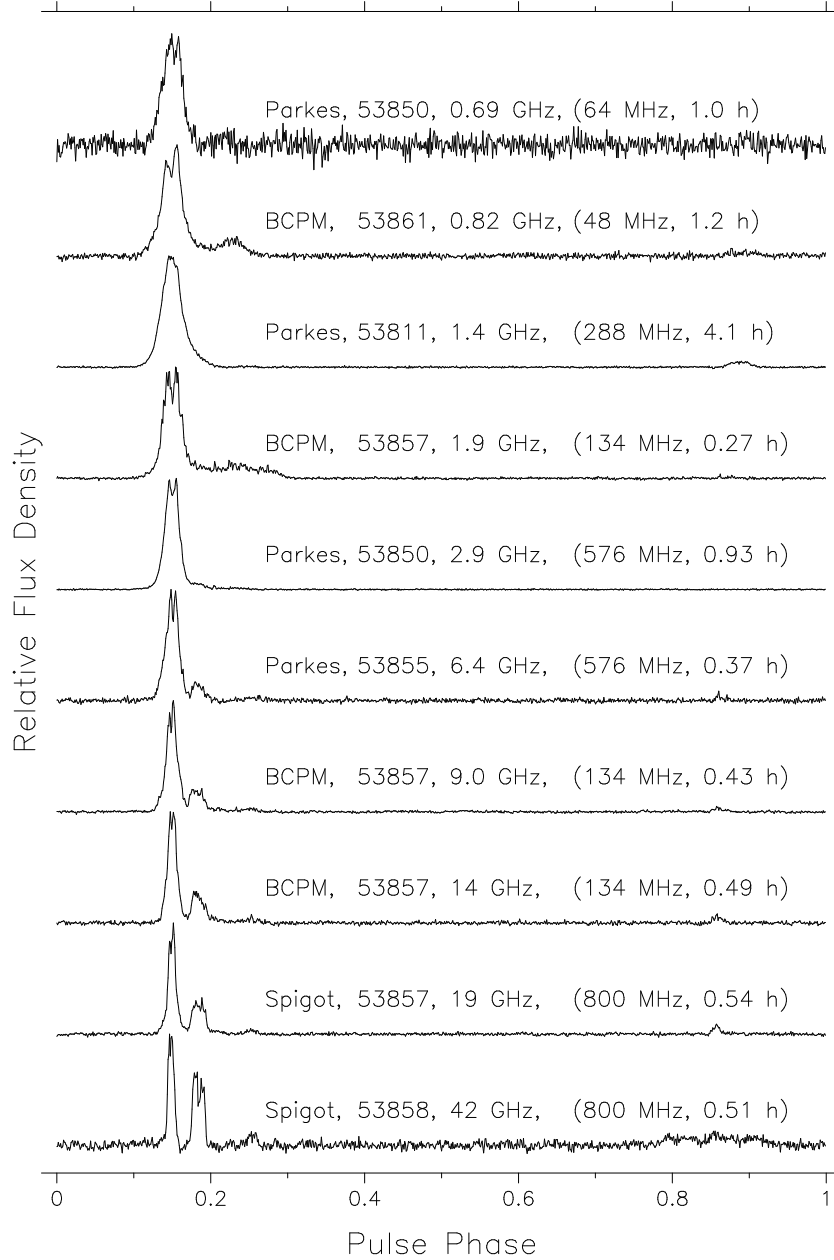


Figure 1. Average radio pulse profiles of XTE J1810–197 at frequencies 0.7–42 GHz. Full-period (5.54 s) profiles are displayed with 1,024-bin resolution in order of ascending frequency from top to bottom, and aligned by fitting the main pulse peak with a gaussian. Above each trace we list the equipment, date (MJD), central frequency, nominal bandwidth, and integration time used to obtain each profile. In some cases a small number of frequency channels corrupted by radio-frequency interference have been omitted in constructing the profiles. The Parkes 1.4-GHz (discovery) observation shows a small pulse preceding the main pulse by about 0.25 in phase. This precursor pulse is not detected on some days. These and other changes may be related to the well-known emission of separate “modes”²⁷ displayed by some ordinary pulsars, or could be more exotic, for instance due to magnetic field reconfiguration or magnetospheric currents varying on timescales of days to weeks. The separation between the two peaks of the main pulse component appears to decrease with increasing frequency, possibly akin to what is observed in some ordinary pulsars, for which the separation is interpreted as reflecting a decreasing emission altitude with increasing frequency. For observations at Parkes we used an analogue filterbank with one-bit digitization and a high-pass filter of time constant ≈ 0.9 s that significantly distorts the measured profiles. We corrected for this using the prescription given in ref. 5. At GBT we used both the BCPM²⁸ and Spigot,²⁹ and no such coarse artefacts resulted.

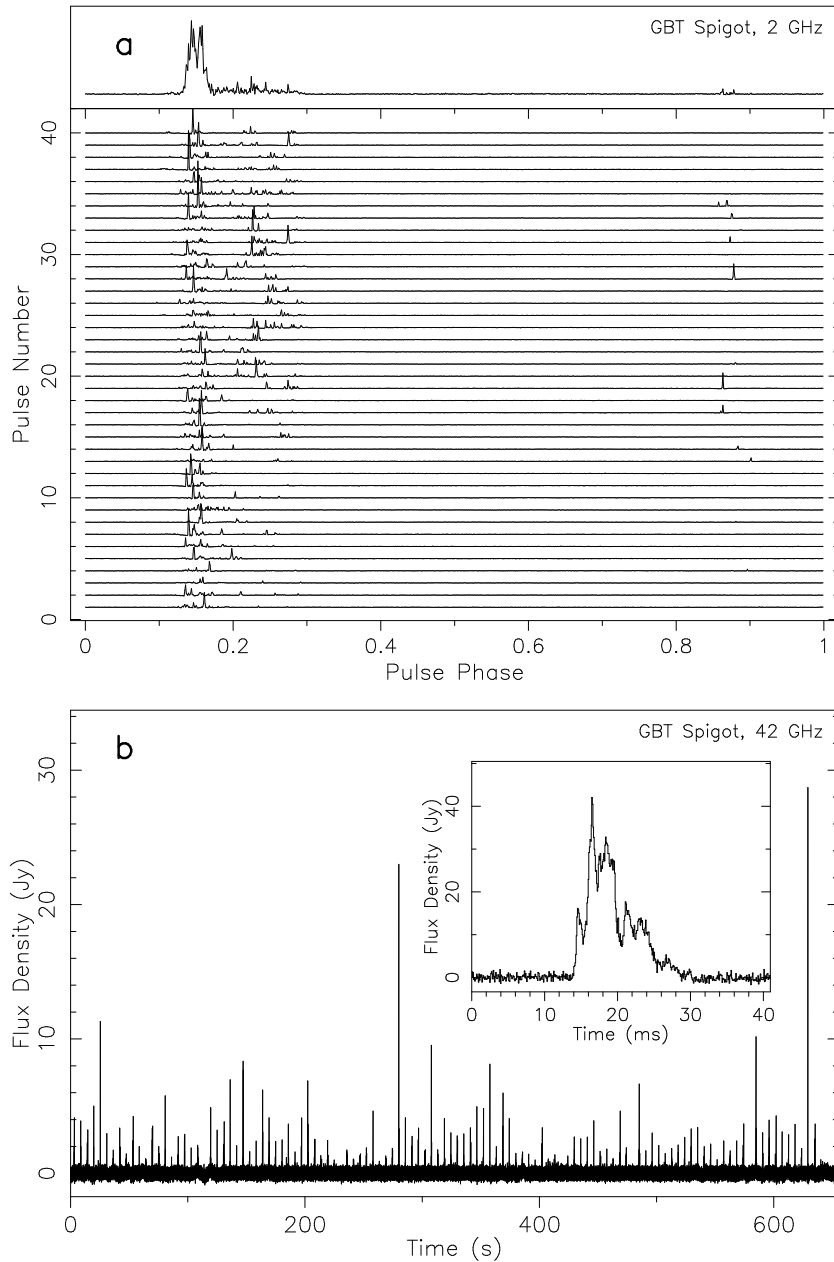


Figure 2. Single pulses from XTE J1810–197 at frequencies of 2 and 42 GHz. We detect single pulses from most rotations of the neutron star irrespective of frequency. **a**, We show here a typical set of 40 consecutive single pulses from our GBT observation at 2 GHz on MJD 53857, where each row represents the full pulse phase displayed with 5.4-ms resolution (1,024 bins). The sum of all 40 pulses is displayed at the top. Sub-pulses (for which we have found no evidence of “drifts”³⁰) with typical width $\lesssim 10$ ms arrive at different phases and gradually build up the average profile — which, however, appears different in observations 8 days later, with the shoulder at phase 0.2–0.3 essentially missing. It is unclear whether this behaviour is similar in detail to what is observed in ordinary pulsars. **b**, A train of about 115 consecutive single pulses detected at a frequency of 42 GHz with the GBT, displayed with 1.3-ms resolution. For display purposes, we have removed large-amplitude power variations with timescales of $\gtrsim 10$ s, probably of atmospheric origin, by high-pass-filtering the data. The flux-density scale is uncertain by a factor of about 2. Inset, a 40-ms-long detail of the brightest pulse from the main panel, displayed with full 81.92- μ s Spigot resolution. The pulse has structure with features as narrow as ≈ 0.2 ms.